

# Analysis of the Photodecomposition Products of $\text{Ru}(\text{bpy})_3^{2+}$ in Various Buffers and upon Zeolite Encapsulation

Anand Vaidyalingam and Prabir K. Dutta\*

Department of Chemistry, The Ohio State University, 120 West 18th Avenue, Columbus, Ohio 43210

**The photodecomposition products of  $\text{Ru}(\text{bpy})_3^{2+}$  in water, in aqueous buffered solutions and encapsulated in zeolite-Y have been analyzed by chromatography and UV–visible spectroscopy. The chromatographic method is found to be capable of separating species with the same charge but slightly different ligands as well as geometrical isomers. In all the systems investigated, photodecomposition proceeded via photoaquation resulting in the formation of *cis*- and *trans*- $\text{Ru}(\text{bpy})_2(\text{OH}_2)_2^{2+}$ . In the case of acetate and phthalate buffers, a third species,  $\text{Ru}(\text{bpy})_2(\text{L})(\text{OH}_2)^+$ , where L is the buffer anion, was found to be the dominant product. For a given pH, the extent of decomposition was found to be dependent on both the buffer anion, following the trend, phosphate < acetate << phthalate and buffer concentration. The presence of the electron-transfer quenching agent, *N,N*-dimethyl-4,4'-bipyridinium ion in the medium led to a decrease of the photodecomposition and closely followed the quenching efficiency as measured by intensity and lifetime quenching studies. Encapsulation of  $\text{Ru}(\text{bpy})_3^{2+}$  in the supercages of zeolite-Y did not lead to a substantial decrease in photodecomposition as compared to an aqueous solution, suggesting that the expected enhanced stability of  $\text{Ru}(\text{bpy})_3^{2+}$  due to the destabilization of  $^3\text{dd}$  orbitals and the cage effect was being negated by the close proximity and intrazeolite packing of  $\text{H}_2\text{O}$  molecules around the Ru center.**

Novel photochemical properties of ruthenium polypyridyl complexes are being extensively exploited in many diverse applications. In analytical chemistry, for example tris(2,2'-bipyridyl)ruthenium(II) ( $\text{Ru}(\text{bpy})_3^{2+}$ ) is being used as a chemiluminescence label for quantitating oxidants such as persulfate and reductants such as amines.<sup>1</sup> Polypyridyl complexes of Ru also find applications as the luminescent probe in oxygen sensors.<sup>2</sup>  $\text{Ru}(\text{bpy})_3^{2+}$  is a popular choice as photosensitizer for photochemical water-splitting systems.<sup>3</sup> In addition,  $\text{Ru}(\text{bpy})_3^{2+}$ -type molecules are also finding increasing use as a building block for the preparation of photoactive supramolecular assemblies.<sup>4–6</sup> Photo-

chemical and photophysical properties of ruthenium(II) polypyridyl complexes have been studied in extensive detail over the past several decades.<sup>7–9</sup> Upon visible excitation, a long-lived metal-to-ligand charge-transfer (MLCT) state is formed, which is usually the state that is involved in the electron transfer, emission, or quenching chemistry.<sup>10</sup> Besides the excited MLCT state, these molecules are often characterized by the presence of thermally accessible excited dd states ( $d\pi^5d\sigma^*1$ ).<sup>11,12</sup>

A problem with the use of ruthenium polypyridyl complexes in photochemical applications is the photoinitiated decomposition arising from the population of the low-lying dd states.<sup>11–14</sup> There are four possible strategies discussed in the literature to minimize the photodecomposition.<sup>10,12</sup> First is the preclusion of solvents of low dielectric constants and strongly ligating anions in the system. The photodissociation involves an intermediate in which the bpy ligand is partially deligated and coordinating anions can complex to the Ru promoting complete deligation.<sup>13,15</sup> The use of aqueous solutions alleviates this problem to some degree, but often the aqueous solutions require the use of buffers. Second is the use of lower temperatures, which via a Boltzmann effect diminishes the population of the low-lying dd states,<sup>11</sup> thereby decreasing photodissociation. However, in analytical applications, experiments at lower temperature may not be practical. Third, for reactions in which a quencher molecule reacts with the MLCT state of  $\text{Ru}(\text{bpy})_3^{2+}$ , increased concentrations of the quencher should diminish the photodissociation chemistry.<sup>10,12</sup> Fourth, the photodecomposition can be alleviated if the dd ligand field state can be destabilized, thus lowering the probability of populating it. It has been proposed that encapsulation in rigid media such as cation-

- (1) Gerardi, R. D.; Barnett, N. W.; Lewis, S. W. *Anal. Chim. Acta* **1999**, *378*, 1–43.
- (2) Wolfbeis, O. S. *Anal. Chem.* **2000**, *72*, 81R–89R.
- (3) Amouyal, E. *Sol. Energy Mater. Sol. Cells* **1995**, *38*, 249–276.
- (4) Yonemoto, E. H.; Saupe, G. B.; Schmehl, R. H.; Hubig, S. M.; Riley, R. L.; Iverson, B. L.; Mallouk, T. E. *J. Am. Chem. Soc.* **1994**, *116*, 4786–4795.

- (5) Benniston, A. C.; Mackie, P. R.; Harriman, A. *Angew. Chem., Int. Ed. Engl.* **1998**, *37*, 354–356.
- (6) Harriman, A.; Hissler, M.; Khatyr, A.; Ziessel, R. *Chem. Commun.* **1999**, 735–736.
- (7) Balzani, V.; Boletta, F.; Gandolfi, M.-T.; Maestri, M. *Top. Curr. Chem.* **1978**, *75*, 1–64.
- (8) Balzani, V.; Moggi, L.; Manfrin, M. F.; Bolletta, F.; Laurence, G. S. *Coord. Chem. Rev.* **1975**, *15*, 321–433.
- (9) Kalyanasundaram, K. *Coord. Chem. Rev.* **1982**, *46*, 159–244.
- (10) Juris, A.; Balzani, V.; Barigelli, F.; Campagna, S.; Belser, P.; Von Zelewsky, A. *Coord. Chem. Rev.* **1988**, *84*, 85–277.
- (11) Van Houten, J.; Watts, R. J. *J. Am. Chem. Soc.* **1976**, *98*, 4853–4858.
- (12) Durham, B.; Caspar, J. V.; Nagle, J. K.; Meyer, T. J. *J. Am. Chem. Soc.* **1982**, *104*, 4803–4810.
- (13) Gleria, M.; Francesco, M.; Beggiato, G.; Bortolus, P. *J. Chem. Soc. Chem. Commun.* **1978**, 285.
- (14) Hoggard, P. E.; Porter, G. B. *J. Am. Chem. Soc.* **1978**, *100*, 1457–1463.
- (15) Van Houten, J.; Watts, R. J. *Inorg. Chem.* **1978**, *17*, 3381–3385.

exchange polymer resins<sup>16</sup> or zeolites<sup>17</sup> should reduce the photolability. The origin of the reduced photolability can arise from destabilization of the dd state as well as the increased probability of bpy ring enclosure due to encapsulation.

Reports on photochemical applications of Ru(bpy)<sub>3</sub><sup>2+</sup> have often relied on absorption spectroscopic study of the photolyzed solutions to estimate the photodegradation.<sup>18</sup> In the case of heterogeneous constrained media such as zeolites, the conclusions regarding ligand loss were inferred from spectroscopic data such as emission lifetimes, changes in resonance Raman frequencies, and temperature-dependent lifetimes via the extent of destabilization of the ligand field state.<sup>17,19</sup> Even when photochemical studies were attempted in rigid media such as poly(methyl methacrylate) (PMMA), there has been no attempt to separate the photoproducts.<sup>20</sup> Spectroscopic methods on unseparated mixtures containing small amounts of decomposition products makes it difficult to identify the photoproducts and the extent of decomposition, especially when the products have spectroscopic properties similar to that of the parent Ru(bpy)<sub>3</sub><sup>2+</sup>. Also, to the best of our knowledge, there has been no study reported in the literature aimed at analyzing the photodegradation products of Ru(bpy)<sub>3</sub><sup>2+</sup> entrapped in a heterogeneous constrained media.

High-performance liquid chromatography (HPLC), especially if employed with diode-array detection, is an ideal tool to study potentially complicated systems. Reverse-phase HPLC has been used for separation and identification of a long-lived intermediate with a monodentate ligand in the photosubstitution of Ru(bpy)<sub>2</sub>(dmbpy)<sup>2+</sup>.<sup>21</sup> Other relevant applications of reverse-phase HPLC include the separation of (1) hydrolysis products of tris(2,2'-bipyridyl)ruthenium(II) derivatives,<sup>22</sup> (2) water reduction products of Ru(bpy)<sub>3</sub><sup>3+</sup>,<sup>23</sup> and (3) spontaneous reduction products of unstable Ru(IV) oxo complexes.<sup>24</sup> Cation-exchange HPLC has also been used for the synthesis and photochemical studies of bis(2,2'-bipyridyl) ruthenium(II) complexes.<sup>25</sup>

Despite the above-mentioned applications of HPLC for the separation and identification of Ru(II) polypyridyl complexes, there has been no systematic study of the fate of Ru(bpy)<sub>3</sub><sup>2+</sup> upon photolysis in different environments. We report here a reverse-phase ion-pair HPLC method to estimate the extent of photodecomposition and to separate and identify the different decomposition products of Ru(bpy)<sub>3</sub><sup>2+</sup>. We have investigated the photolysis of Ru(bpy)<sub>3</sub><sup>2+</sup> in solution media with a set of commonly used buffers, in the presence of an electron-transfer quenching agent, and encapsulated in the supercages of zeolite Y. We conclude that

the photodecomposition is strongly dependent on the buffer and can be decreased significantly by efficient quenching of the excited state.

## EXPERIMENTAL SECTION

**Synthesis.** The nanocrystalline zeolite-Y was synthesized, following a patent literature procedure, from aqueous silicate (27% SiO<sub>2</sub> in 14% NaOH, Sigma) and aluminate (Na<sub>2</sub>Al<sub>2</sub>O<sub>4</sub>·3H<sub>2</sub>O, Chem Service) solutions with a molar ratio of SiO<sub>2</sub>/Al<sub>2</sub>O<sub>3</sub> ~ 6.<sup>26</sup> Intrazeolitic synthesis of tris(2,2'-bipyridyl)ruthenium(II) inside the supercages of nanocrystalline zeolite-Y was carried out according to literature method and was found to contain 33.6 μmol of Ru(bpy)<sub>3</sub><sup>2+</sup>/g of zeolite, or ~1 complex/15 supercages.<sup>27</sup> Silylation of the zeolitic surface of Ru(bpy)<sub>3</sub><sup>2+</sup> containing nanocrystals was accomplished using *n*-octadecyltrichlorosilane (OTS; 95% Aldrich) in toluene (AR, Mallinckrodt).<sup>28</sup>

**Photolysis.** A model A1010 xenon arc lamp equipped with a LPS 250 power supply (Photon Technology International) was used for photolysis experiments. A 3-in.-long water filter and a 420-nm glass cutoff filter were used to remove IR and UV radiation, respectively, and the radiation was reflected off a mirror that reflects light in the range 420–650 nm and focused to a 1-cm spot. The power of the incident radiation as measured using a Coherent 210 power meter was found to be ~300 mW/cm<sup>2</sup>. Sodium phosphate monobasic hydrate (ACS, Fischer), sodium phosphate dibasic dodecahydrate (Baker analyzed), sodium acetate trihydrate (Jenneile), glacial acetic acid (Mallinckrodt), potassium hydrogen phthalate (Baker analyzed), and sodium hydroxide (AR, Mallinckrodt) were used in the preparation of buffers in Nanopure water (18 MΩ cm<sup>-1</sup>).

Photolysis reactions were carried out either in buffer solutions of given pH and concentration or in distilled water containing 2 × 10<sup>-4</sup> M Ru(bpy)<sub>3</sub><sup>2+</sup>. In the case of zeolite-entrapped Ru(bpy)<sub>3</sub><sup>2+</sup>, the hydrophobic silylated particles were suspended in toluene to get an optically clear 2 × 10<sup>-4</sup> M in Ru(bpy)<sub>3</sub><sup>2+</sup> solution. In all cases, 5 mL of the solution in a modified spectrophotometric quartz cell (1 cm path length) was purged with nitrogen gas for 45 min and was photolyzed for 8 h, under stirring. Solution absorption spectra were recorded and HPLC separation was carried out, before and immediately after photolysis. For chromatographic analysis of the zeolite sample, the toluene suspension was centrifuged and the separated solid zeolite particles were treated with citric acid (Jenneile Enterprises) to extract the zeolite-entrapped complexes.<sup>29</sup> *cis*-Dichlorobis(2,2'-bipyridine)ruthenium(II) dihydrate was obtained from Strem Chemicals.

**Instrumentation.** Absorbance measurements were carried out using a Shimadzu model UV-265 spectrophotometer. A Corning model 125 pH meter with a general purpose combination electrode was used for all pH measurements. A Shimadzu high-performance liquid chromatograph equipped with a model FCV-10ALvp low-pressure gradient flow controller, model DGU-14A on-line degasser, model LC10-ATvp pump, model SPD-M10Avp diode-array absorbance detector (standard 10-mm optical path length cell), and 30 cm × 3.9 mm i.d. μBondapak ODS column (Waters

(16) Masschelein, A.; Mesmaeker, A. K.-D.; Willsher, C. J.; Wilkinson, F. J. *Chem. Soc., Faraday Trans.* **1991**, *87*, 259–267.

(17) Maruszewski, K.; Kincaid, J. R. *Inorg. Chem.* **1995**, *34*, 2002–2006.

(18) Kleijn, J. M.; Rouwendal, E.; Van Leeuwen, H. P.; Lyklema, J. J. *Photochem. Photobiol., A* **1988**, *44*, 29–50.

(19) Maruszewski, K.; Strommen, D. P.; Kincaid, J. R. *J. Am. Chem. Soc.* **1993**, *115*, 8345–8350.

(20) Adelt, M.; Devenney, M.; Meyer, T. J.; Thompson, D. W.; Treadway, J. A. *Inorg. Chem.* **1998**, *37*, 2616–2617.

(21) Tachiyashiki, S.; Ikezawa, H.; Mizumachi, K. *Inorg. Chem.* **1994**, *33*, 623–625.

(22) Valenty, S. J.; Behnken, P. E. *Anal. Chem.* **1978**, *50*, 834–837.

(23) Ghosh, P. K.; Brunschwig, B. S.; Chou, M.; Creutz, C.; Sutin, N. *J. Am. Chem. Soc.* **1984**, *106*, 4772–4783.

(24) Roecker, L.; Kutner, W.; Gilbert, J. A.; Simmons, M.; Murray, R. W.; Meyer, T. J. *Inorg. Chem.* **1985**, *24*, 3784–3791.

(25) Buchanan, B. E.; McGovern, E.; Harkin, P.; Vos, J. G. *Inorg. Chim. Acta* **1988**, *154*, 1–4.

(26) Ambs, W. J. U.S. Patent, 4,372,931, 1983.

(27) Castagnola, N. B.; Dutta, P. K. *J. Phys. Chem. B* **1998**, *102*, 1696–1702.

(28) Singh, R.; Dutta, P. K. *Microporous Mesoporous Mater.* **1999**, *32*, 29–35.

(29) Maruszewski, K.; Strommen, D. P.; Handrich, K.; Kincaid, J. R. *Inorg. Chem.* **1991**, *30*, 4579–4582.

Associates) was used for the separation studies. Samples were injected through a Rheodyne 7725i injector equipped with a 10- $\mu$ L sample loop.

**Separation.** Separations were carried out with a binary gradient using methanol (A) (Fischer Optima) and pH 5, 0.025 M phosphate buffer (B), both containing  $5 \times 10^{-3}$  M 1-heptane-sulfonic acid sodium salt (Puriss, Fluka) as ion-pairing agent with a flow rate of 1.0 mL/min. Optimum separation was achieved with a 12-min linear gradient from 20% A to 80% A and held for 8 min. Equilibration time between runs was 10 min. The separated components were detected by their absorption spectrum (190–600 nm), and the chromatogram were recorded at given wavelengths. Calibration was carried out with five standards of  $\text{Ru}(\text{bpy})_3^{2+}$  of known concentration in the range of  $1 \times 10^{-3}$ – $1 \times 10^{-5}$  M. Three independent injections of the standards were carried out and the average was employed. The peak area as a function of concentration was found to be linear ( $r^2 = 0.999$ ), and this calibration curve was used to estimate the extent of  $\text{Ru}(\text{bpy})_3^{2+}$  decomposition.

## RESULTS

**Aquation Chemistry of  $\text{Ru}(\text{bpy})_2\text{Cl}_2$ .** A known amount of  $\text{Ru}(\text{bpy})_2\text{Cl}_2$  was suspended in water and stirred for  $\sim 30$  min under  $\text{N}_2$  atmosphere shielded from ambient light. The clear solution obtained after centrifugation was used for further analysis. Upon chromatographic separation, peaks were noted with retention times of 12.5 (peak 1) and 13.4 min (peak 2). Photolysis of the aqueous solution of  $\text{Ru}(\text{bpy})_2\text{Cl}_2$  resulted in increase of the intensity of peak 1 and the resulting chromatogram is shown in Figure 1A. These intensities could be reversed by heating, without any changes in the absorption spectra. The absorption spectra of species 1 exhibited bands at 296, 352, and 498 nm, whereas species 2 has bands at 292,  $\sim 350$ , and 486 nm.

**Photoaquation Chemistry of  $\text{Ru}(\text{bpy})_3^{2+}$ .** (i) **Water.** Photolysis of  $\text{Ru}(\text{bpy})_3^{2+}$  in distilled water ( $2 \times 10^{-4}$  M) for 8 h showed very little change in the solution absorption spectra, with slight broadening of the lowest energy absorption at 450 nm. The solution after 8 h of photolysis was analyzed by HPLC and the chromatogram is shown in Figure 1B. The peak marked R in the chromatogram eluting at 16.5 min exhibited a spectrum identical to  $\text{Ru}(\text{bpy})_3^{2+}$  and eluted at the same retention time as the unphotolyzed sample. The two peaks 1 and 2 in the chromatogram after photolysis were similar in retention time and absorption spectra to those obtained in the case of  $\text{Ru}(\text{bpy})_2\text{Cl}_2$ . The area of the  $\text{Ru}(\text{bpy})_3^{2+}$  (peak R) decreased upon photolysis by 6% as compared to the unphotolyzed sample. Inspection of the chromatogram monitored at 282 nm revealed the presence of a fourth peak with retention time of  $\sim 13$  min and absorption spectrum identical to that of authentic bipyridine.

(ii) **Buffer.** Photolysis of  $2 \times 10^{-4}$  M  $\text{Ru}(\text{bpy})_3^{2+}$  solutions in pH 5 acetate buffer with concentrations of acetate of 0.025, 0.1, and 2 M were also carried out. After 8 h of photolysis, the lowest energy absorption at 450 nm decreased and a shoulder at  $\sim 500$  nm appeared. This was most marked with the 2 M buffer whose absorption spectrum before and after photolysis is compared in Figure 2A. The chromatograms obtained with the photolyzed solution with the 2 M buffer are shown in Figure 1C. Three photoproducts labeled 1–3 with retention times of 12.5, 13.4, and 14.1 min, respectively, along with peak R due to  $\text{Ru}(\text{bpy})_3^{2+}$  were

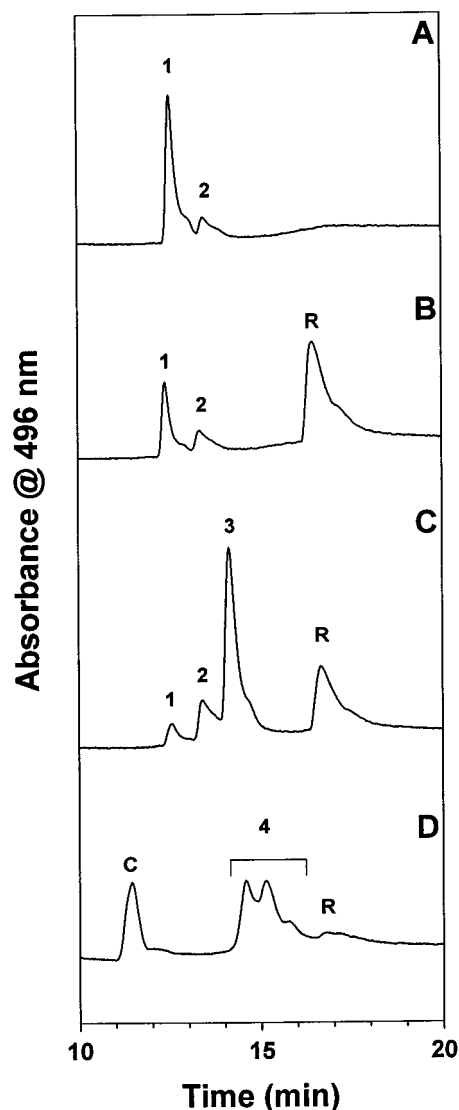


Figure 1. HPLC traces of (A) saturated aqueous solution of  $\text{Ru}(\text{bpy})_2\text{Cl}_2$  after photolysis, (B) Photolyzed solution of  $2 \times 10^{-4}$  M  $\text{Ru}(\text{bpy})_3^{2+}$  in distilled water, (C) Photolyzed solution of  $2 \times 10^{-4}$  M  $\text{Ru}(\text{bpy})_3^{2+}$  in 2 M acetate buffer (pH 5) (D) Photolyzed solution of  $2 \times 10^{-4}$  M  $\text{Ru}(\text{bpy})_3^{2+}$  and  $[\text{Co}(\text{NH}_3)_5\text{Cl}]^{2+}$  (all data are being shown with the same y-axis absorbance scale; all photolysis carried out for 8 h).

identified. Peaks 1 and 2 were similar in retention times and spectra to those in Figure 1A, and the spectrum of the peak labeled 3 is shown in Figure 2B, with bands at 292, 350, and 496 nm. The increase in the relative proportion of peak 3 was found to be directly dependent on the acetate buffer concentration. The peak due to  $\text{Ru}(\text{bpy})_3^{2+}$  diminished with increasing acetate concentration. The extent of decomposition of  $\text{Ru}(\text{bpy})_3^{2+}$  as estimated from the HPLC traces were 12, 18, and 50% in 0.025, 0.10, and 2 M acetate buffers, respectively. Table 1 compares the extent of photodecomposition. Photolysis of  $\text{Ru}(\text{bpy})_3^{2+}$  solution in 0.025 M, pH 5 phosphate buffer showed the same two photoproducts (1) and (2) as shown in Figure 1A and the extent of  $\text{Ru}(\text{bpy})_3^{2+}$  decomposition was 8%. The chromatogram with the 0.025 M potassium hydrogen phthalate (KHP/NaOH) buffer showed a broad peak around the retention time for species 2. Cross sections of the absorption spectra at various positions along peak 2 showed



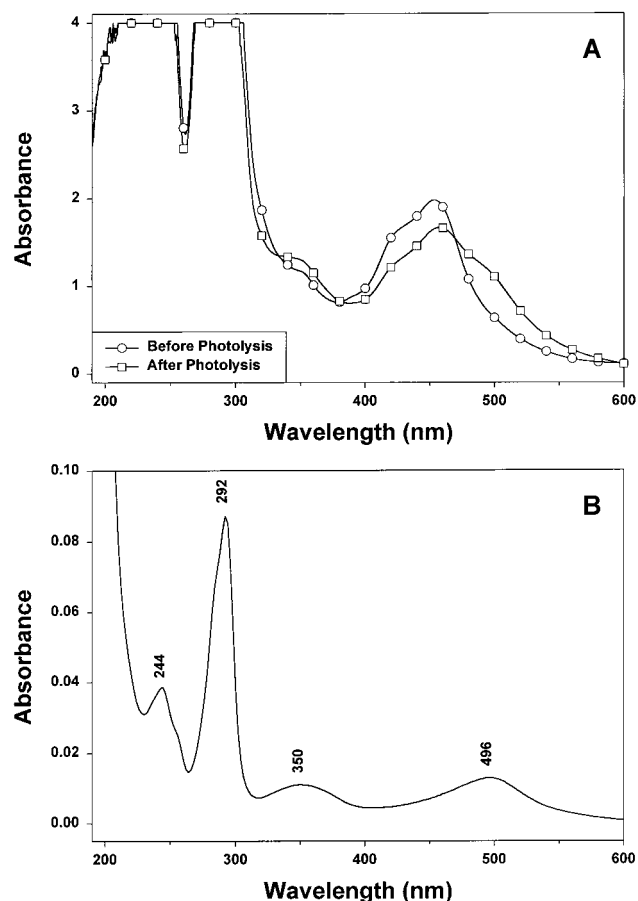


Figure 2. (A) Absorption spectra of  $2 \times 10^{-4}$  M  $\text{Ru}(\text{bpy})_3^{2+}$  in 2 M acetate buffer (pH 5) before and after 8 h of photolysis. (B) Absorption spectrum of peak 3 in Figure 1C.

Table 1. Fraction of  $\text{Ru}(\text{bpy})_3^{2+}$  Lost during 8-h Photolysis under Various Conditions

medium	buffer concn (M)	pH	fraction loss <sup>a</sup>
acetate	2.0	4.0	0.60
acetate	2.0	5.0	0.50
acetate	0.10	5.0	0.18
acetate	0.025	5.0	0.12
phthalate	0.025	5.0	0.42
phosphate	0.025	5.0	0.08
phosphate	2.0	5.0	0.13
water			0.06
zeolite			0.06

<sup>a</sup> Defined as loss of  $\text{Ru}(\text{bpy})_3^{2+}$  upon photolysis relative to the original sample.

that it is a mixture of two components. The absorption spectrum of the new component that is distinct from species 2 has absorption bands at 294, 356, and 510 nm. The extent of  $\text{Ru}(\text{bpy})_3^{2+}$  decomposition in the phthalate buffer system as measured by the decrease in peak R was 42%.

The effect of pH on the photodecomposition of  $\text{Ru}(\text{bpy})_3^{2+}$  was studied by employing 2 M, pH 5 and pH 4 acetate buffers. At the lower pH, the same three decomposition products as observed at the higher pH were obtained, though the decomposition of  $\text{Ru}(\text{bpy})_3^{2+}$  was enhanced to 60%.

**(iii) Zeolite-Encapsulated  $\text{Ru}(\text{bpy})_3^{2+}$ .** Zeolite encapsulation affords the opportunity to examine the photodecomposition of  $\text{Ru}(\text{bpy})_3^{2+}$  in a constrained medium. Moreover, since the charge

Table 2. Fraction of  $\text{Ru}(\text{bpy})_3^{2+}$  Lost during 8-h Photolysis in the Presence of  $\text{MV}^{2+}$  (2 M Acetate Buffer, pH 5)

$\text{MV}^{2+}$ concn (M)	fraction loss <sup>a</sup>	decrease in photodecomp <sup>b</sup> (%)	quenching efficiency, $\phi_q^c$ (%)
0	0.50	0	0
$4 \times 10^{-4}$	0.47	7	23
$2 \times 10^{-3}$	0.23	54	62
$4 \times 10^{-3}$	0.12	77	76
$6 \times 10^{-3}$	0.07	85	83
$1 \times 10^{-2}$	0.07	86	89

<sup>a</sup> Defined as loss of  $\text{Ru}(\text{bpy})_3^{2+}$  upon photolysis relative to the original sample. <sup>b</sup> Defined as  $(D_0 - D)/D_0$ , where  $D_0$  is the fraction lost in the absence of  $\text{MV}^{2+}$  and  $D$  is the fraction lost in the presence of given concentration of  $\text{MV}^{2+}$  (pH 5, 2 M acetate buffer). <sup>c</sup>  $\Phi_q = 100K_{sv}[\text{Q}]/(1 + K_{sv}[\text{Q}])$  calculated with  $K_{sv} = 820 \text{ M}^{-1}$  (obtained from intensity and lifetime quenching).

neutralization of the  $\text{Ru}(\text{bpy})_3^{2+}$  occurs by the charge on the zeolite framework, there are no coordinating anions present. Use of rigid media like zeolite crystals normally would preclude the use of solution medium for any meaningful photochemical studies, often requiring a pressed pellet wherein only the surface could be sampled. By silylating the surface of the nanocrystalline zeolite-Y crystals containing  $\text{Ru}(\text{bpy})_3^{2+}$ , we were able to render these crystals highly hydrophobic. These hydrophobic crystals could be suspended in organic media such as toluene, and it was found that at least 80% of the encapsulated complexes could be spectroscopically sampled.<sup>30</sup> It is important to note that though the medium is organic, the immediate vicinity of  $\text{Ru}(\text{bpy})_3^{2+}$  inside the supercages contains plenty of water molecules. Employing these relatively clear nanocrystallite suspensions allows us to quantitatively compare the photodecomposition of  $\text{Ru}(\text{bpy})_3^{2+}$  in aqueous solution directly with that in the zeolite. Photolysis of the toluene suspension followed by the extraction of the encapsulated complexes into aqueous solution showed the same HPLC peaks as with aqueous  $\text{Ru}(\text{bpy})_3^{2+}$  with comparable amounts of  $\text{Ru}(\text{bpy})_3^{2+}$  destruction of the order of 6%.

**(iv) Photodecomposition of  $\text{Ru}(\text{bpy})_3^{2+}$  in the Presence of a Quencher.** One of the most extensively studied reactions of  $\text{Ru}(\text{bpy})_3^{2+}$  is electron transfer from the photoexcited state to quencher molecules. In particular, bipyridinium ions have been extensively studied for oxidative quenching. We examined the photodecomposition of  $2 \times 10^{-4}$  M  $\text{Ru}(\text{bpy})_3^{2+}$  in a 2 M acetate buffer (pH 5) in the presence of *N,N*-dimethyl-4,4'-bipyridinium ion (methylviologen,  $\text{MV}^{2+}$ ), at concentrations up to  $1 \times 10^{-2}$  M. Typical studies reported in the literature have used concentration of  $\text{MV}^{2+}$  ranging from  $1.5 \times 10^{-5}$  to  $3 \times 10^{-3}$  M for photochemical  $\text{H}_2$  evolution experiments.<sup>3,18</sup> The same three decomposition products as obtained with the acetate buffer (Figure 1C) were also observed in the presence of  $\text{MV}^{2+}$ . Table 2 shows the extent of decomposition of  $\text{Ru}(\text{bpy})_3^{2+}$  as a function of  $\text{MV}^{2+}$  concentration and ranges from 50% in the absence of  $\text{MV}^{2+}$  to 7% for  $\text{MV}^{2+}$  concentrations of  $1 \times 10^{-2}$  M. It is clear that, with very high concentrations of  $\text{MV}^{2+}$ , the decomposition of  $\text{Ru}(\text{bpy})_3^{2+}$  can be almost completely suppressed and is comparable to that in distilled

(30) Castagnola, N. B. Ph.D. Dissertation, The Ohio State University, Columbus, OH, 1999; pp 169–210.

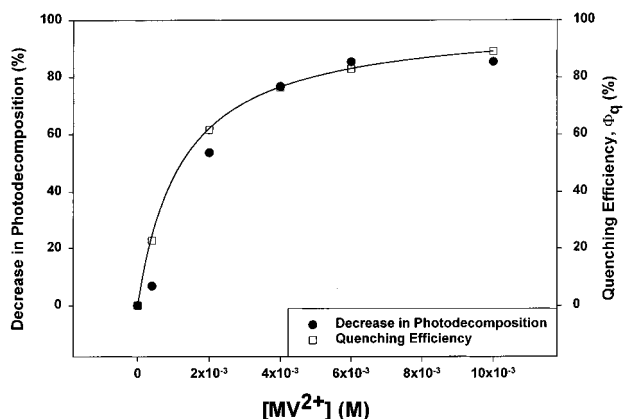


Figure 3. Plot comparing the decrease in photodecomposition of  $\text{Ru}(\text{bpy})_3^{2+}$  in 2 M acetate buffer (pH 5) with the quenching efficiency by  $\text{MV}^{2+}$  (solid line is the fit using the expression for  $\phi_q$  in Table 2).

water. From the intensity and lifetime quenching of the  $\text{Ru}(\text{bpy})_3^{2+}$  by the  $\text{MV}^{2+}$ , we estimated the quenching efficiency and the data are shown in Table 2. There is a close correlation between the decrease of photodecomposition of  $\text{Ru}(\text{bpy})_3^{2+}$  in the presence of  $\text{MV}^{2+}$  and the quenching efficiency by the  $\text{MV}^{2+}$ , and this is also evident from the plot in Figure 3. The solid line is the fit using  $\phi_q$  from Table 2 with  $K_{\text{SV}} = 820 \text{ M}^{-1}$ .

**Photostability of  $\text{Ru}(\text{bpy})_3^{3+}$ .** To ensure that the decomposition products that we are observing are indeed due to  $\text{Ru}(\text{bpy})_3^{2+}$ , we examined the products formed upon photolysis of  $\text{Ru}(\text{bpy})_3^{3+}$ .  $\text{Ru}(\text{bpy})_3^{3+}$  was generated by excited-state electron-transfer quenching of  $\text{Ru}(\text{bpy})_3^{2+}$  by  $[\text{Co}(\text{NH}_3)_5\text{Cl}]^{2+}$  in 2 M acetate buffer at pH 4.0. Figure 1D shows the HPLC traces after photolysis. The peak identified as (C) is due to  $[\text{Co}(\text{NH}_3)_5\text{Cl}]^{2+}$ , and the peak due to  $\text{Ru}(\text{bpy})_3^{2+}$  (R) has almost disappeared after photolysis. The major decomposition products (labeled 4) were all characterized by strong MLCT charge-transfer bands around 450 nm, indicating that they were formed by modifications of the bpy ligand of  $\text{Ru}(\text{bpy})_3^{2+}$ , as had been postulated by Ghosh et al.<sup>23</sup>

## DISCUSSION

The chromatographic method used in this study is capable of separating not only complexes that differ in their net charge but, more importantly, species that have the same charge with slightly different ligands as well as geometrical isomers. This is evident from the studies on both  $\text{Ru}(\text{bpy})_3^{3+}$  and  $\text{Ru}(\text{bpy})_2\text{Cl}_2$ . For  $\text{Ru}(\text{bpy})_3^{3+}$ , the column readily separated decomposition products that contain modified bipyridyl ligands, since all species showed the MLCT band at 450 nm. In the case of  $\text{Ru}(\text{bpy})_2\text{Cl}_2$ , geometrical isomers could be distinguished.  $\text{Ru}(\text{bpy})_2\text{Cl}_2$  is sparingly soluble in water and is well known to be substitutionally labile, with both the  $\text{Cl}^-$  ions being replaced by the solvent molecules yielding  $\text{Ru}(\text{bpy})_2(\text{OH}_2)_2^{2+}$ .<sup>31</sup> In fact, this procedure is a common synthetic route for  $\text{Ru}(\text{bpy})_2\text{XY}^{n+}$ -type molecules.<sup>32</sup>  $\text{Ru}(\text{bpy})_2(\text{OH}_2)_2^{2+}$  is also known to undergo cis–trans photoisomerization yielding a trans-rich photostationary state with thermal conversion of trans to cis.<sup>33</sup> HPLC separation of this system indeed shows a chromatogram

with two peaks (Figure 1A), and comparison of their absorption spectra with the literature suggest that the peaks labeled 1 and 2 are due to that of *trans*- and *cis*- $\text{Ru}(\text{bpy})_2(\text{OH}_2)_2^{2+}$ , respectively.<sup>33</sup> The ratio of the intensity of the bands due to *trans*:*cis* increased with photolysis and could be reversed by heat treatment, as expected from previous studies.<sup>33</sup>

Photolability of  $\text{Ru}(\text{bpy})_3^{2+}$  in solution is well studied and is found to be facile especially in the presence of small coordinating anions<sup>11,15</sup> or in organic media.<sup>12–14,34</sup> For example, in solvents such as  $\text{CH}_2\text{Cl}_2$ , it is well known that when the counterion is  $\text{Cl}^-$ ,  $\text{Ru}(\text{bpy})_3^{2+}$  is much more prone to photodechelation than when  $\text{PF}_6^-$  salt is employed.<sup>12</sup> The mechanism of the photodecomposition is thought to proceed through population of the thermally accessible <sup>3</sup>dd, which leads to a Ru–N bond lengthening resulting in dechelation and photosubstitution by the ion-paired counteranion. The intermediate in this process is thought to involve a five-coordinate complex with one of the bpy ligands attached via only one of the nitrogens.

At the submillimolar concentrations of  $\text{Ru}(\text{bpy})_3^{2+}$  examined in this study, photolysis of an aqueous  $[\text{Ru}(\text{bpy})_3^{2+}]\text{Cl}_2$  led to the formation of two decomposition products, which on basis of retention times and absorption spectra were identified as *trans*- and *cis*- $\text{Ru}(\text{bpy})_2(\text{OH}_2)_2^{2+}$ . The photochemistry occurring in aqueous solutions is therefore photoaquation, resulting in the formation of *cis*- $\text{Ru}(\text{bpy})_2(\text{OH}_2)_2^{2+}$ , which can undergo photoisomerization to *trans*- $\text{Ru}(\text{bpy})_2(\text{OH}_2)_2^{2+}$ . This is also supported by the presence of small quantities of free bipyridine in the photolyzed solution. After 8 h of photolysis, ~6%  $\text{Ru}(\text{bpy})_3^{2+}$  decomposition was observed. We propose that the chloride ion is not playing a role in forming a substitutionally labile complex considering the low concentrations of the  $\text{Cl}^-$  and that the bpy ligand replacement is occurring directly via water attack. It is also obvious from Figure 1D that the intermediate formation of  $\text{Ru}(\text{bpy})_3^{3+}$  is not involved in the  $\text{Ru}(\text{bpy})_3^{2+}$  photochemistry, since the photodecomposition products of  $\text{Ru}(\text{bpy})_3^{3+}$  are entirely different.

Most photocatalytic studies using  $\text{Ru}(\text{bpy})_3^{2+}$  use buffers of pH in the range of 4–5. From the literature, it is clear that acetate buffer is the medium of choice.<sup>3,18</sup> Another effective buffer in this pH range is KHP/NaOH. We have examined the decomposition pattern of  $\text{Ru}(\text{bpy})_3^{2+}$  in both these buffers. HPLC showed the presence of three peaks. On the basis of the absorption spectra of the separated components, it was clear that two of these peaks were due to *trans*- and *cis*- $\text{Ru}(\text{bpy})_2(\text{OH}_2)_2^{2+}$ . The third peak had the longest wavelength band at 496 and 510 nm for the acetate and phthalate, respectively. In addition, the abundance of the third peak in acetate buffer was found to be directly dependent on the acetate ion concentration, suggesting that it contains acetate as a ligand.<sup>24</sup> We propose that the third species has the form *cis*- $\text{Ru}(\text{bpy})_2(\text{L})(\text{OH}_2)^+$ , where L is the acetate or the monodentate phthalate ion. The shift of the band from 486 nm in the *cis* bis-aquo complex to 496 and 510 nm upon replacing one of the  $\text{H}_2\text{O}$  ligands by acetate and phthalate, respectively, is consistent with the better  $\pi$ -donating character of the carboxylate ligand.<sup>14,15</sup> The bidentate phthalate or two acetate ligands would lead to the formation of a neutral complex and would have precipitated out. We found no evidence of any solid formation during the photolysis reaction.

(31) Davies, N. R.; Mullins, T. L. *Aust. J. Chem.* **1967**, *20*, 657–668.

(32) Wallace, W. M.; Hoggard, P. E. *Inorg. Chem.* **1979**, *18*, 2934–2935.

(33) Durham, B.; Wilson, S. R.; Hodgson, D. J.; Meyer, T. J. *J. Am. Chem. Soc.* **1980**, *102*, 600–607.

(34) Durham, B.; Walsh, J. L.; Carter, C. L.; Meyer, T. J. *Inorg. Chem.* **1980**, *19*, 860–865.

Photodecomposition was also examined in a 0.025 M phosphate buffer at pH 5 and found to be on the order of 8%. Phosphate buffers are not good choices for this pH range, but they do tend to minimize photodecomposition. For a similar buffer concentration with KHP, decomposition is as high as 42%. Hence, it can be concluded that, for a given pH and concentration of buffer, decomposition follows the trend, phosphate < acetate  $\ll$  KHP/NaOH. Lowering the buffer pH to 4 enhances the decomposition of Ru(bpy)<sub>3</sub><sup>2+</sup> up to 60% and is consistent with what is known in the literature.<sup>15</sup>

For reactions involving photoexcited Ru(bpy)<sub>3</sub><sup>2+</sup>, such as electron-transfer quenching with methylviologen, the photodecomposition is minimized. However, as seen from Table 2, it takes a high concentration of MV<sup>2+</sup> ( $1 \times 10^{-2}$  M) to bring down the level of photodecomposition of Ru(bpy)<sub>3</sub><sup>2+</sup> in 2 M acetate buffer to the order of 7%. More typical photolysis conditions involve concentrations of MV<sup>2+</sup> 1 or 2 orders of magnitude lower,<sup>3,18</sup> which would lead to significant photodecomposition of Ru(bpy)<sub>3</sub><sup>2+</sup> in buffers. Table 2 and Figure 3 show that the decrease in photodecomposition has the same trend as the quenching efficiency by the methylviologen.

The effect of Ru(bpy)<sub>3</sub><sup>2+</sup> encapsulation in constrained media on photodecomposition was studied by employing nanocrystalline zeolite-Y crystals containing Ru(bpy)<sub>3</sub><sup>2+</sup>. It can be expected that zeolite encapsulation should promote stability for the following reasons: (1) the zeolite encapsulation is shown to destabilize the <sup>3</sup>dd level,<sup>17,19,35</sup> (2) the absence of photodechelation promoting, small, coordinating anions inside the zeolite, and (3) the cage structure is expected to help in ligand rebinding.<sup>20</sup> The charge neutralization of Ru(bpy)<sub>3</sub><sup>2+</sup> in the zeolite is by the framework aluminate ions, which have no mobility, and considering that the Ru is at the center of the  $\sim 13$ -Å supercage, the aluminates cannot complex the ruthenium. Thus, bpy ligand replacement can only be mediated by intrazeolitic H<sub>2</sub>O molecules. The comparable photochemical decomposition between Ru(bpy)<sub>3</sub><sup>2+</sup> in distilled water and in zeolite suggests that the proposed destabilization of the <sup>3</sup>dd level in the zeolite as well as the rigid cage that should promote the annealing of the intermediate monodentate bpy ligand does not appear to be diminishing the photodecomposition. This may have to do with the nature of intrazeolitic water. In the zeolite, there are 2–4 H<sub>2</sub>O molecules wedged between the bpy ligands and they are well positioned to promote the ligand replacement reaction. The analogy of the intrazeolitic environment can be made with accelerated photodecomposition of Ru(bpy)<sub>3</sub><sup>2+</sup> in organic

solvents where small molecules and ions such as H<sub>2</sub>O and Cl<sup>−</sup> are wedged between the bpy ligands and available to bond to Ru once dechelation of bpy occurs.<sup>12,24</sup> So, in the zeolite, the enhanced stability of Ru(bpy)<sub>3</sub><sup>2+</sup> due to the destabilization of <sup>3</sup>dd orbitals and the cage effect is being negated by the close proximity and packing of H<sub>2</sub>O molecules around the Ru center.

## CONCLUSIONS

The photolability of Ru(bpy)<sub>3</sub><sup>2+</sup> in aqueous and heterogeneous media was studied by reverse-phase ion-pair HPLC, and separation of the photodecomposition products from the starting Ru(bpy)<sub>3</sub><sup>2+</sup> was achieved. Comparison of these chromatographic profiles with that of aqueous Ru(bpy)<sub>2</sub>Cl<sub>2</sub> showed that the common products are *cis*- and *trans*-Ru(bpy)<sub>2</sub>(OH)<sub>2</sub><sup>2+</sup>. In the case of acetate and phthalate buffers, a third species was found and, on the basis of the absorption spectra and concentration dependence on the buffer anion, was identified as Ru(bpy)<sub>2</sub>(L)(OH)<sub>2</sub><sup>+</sup>, where L is acetate or phthalate. It can be concluded that, for a given pH and concentration of buffer, Ru(bpy)<sub>3</sub><sup>2+</sup> decomposition follows the trend, phosphate < acetate  $\ll$  phthalate. Addition of *N,N'*-methyl-4,4'-bipyridinium ion to quench Ru(bpy)<sub>3</sub><sup>2+</sup> led to a decrease in the decomposition. But under typical conditions found in the literature involving MV<sup>2+</sup> concentrations of less than  $1 \times 10^{-2}$  M, significant photodecomposition of Ru(bpy)<sub>3</sub><sup>2+</sup> will still occur if buffers are used. The photodecomposition pattern of the Ru(bpy)<sub>3</sub><sup>2+</sup> encapsulated in nanocrystalline zeolite-Y crystals indicates that the enhanced stability of Ru(bpy)<sub>3</sub><sup>2+</sup> due to the destabilization of <sup>3</sup>dd orbitals and the cage effect is being negated by the close proximity and packing of H<sub>2</sub>O molecules around the Ru center.

## ACKNOWLEDGMENT

We gratefully acknowledge the financial support of DOE, Basic Energy Sciences for this research. We are thankful to Mr. Todd Rittenhouse for helpful discussions regarding HPLC and to Dr. Norma Castagnola for the synthesis of nanocrystalline Ru(bpy)<sub>3</sub><sup>2+</sup>-zeolite-Y.

## SUPPORTING INFORMATION AVAILABLE

Absorption spectra and chromatograms of several of the photolysis systems. This material is available free of charge via the Internet at <http://pubs.acs.org>.

Received for review April 10, 2000. Accepted August 9, 2000.

AC000408E

(35) Bhuiyan, A. A.; Kincaid, J. R. *Inorg. Chem.* **1998**, *37*, 2525–2530.